J. Indian Chem. Soc.,
Vol. 94, January 2017, pp. 83-93

Effects of interaction between non-steroidal anti-inflammatory drugs with BSA and DNA base : Spectral, electrochemical and molecular docking methods

N. Rajendiran* and J. Thulasidhasan

Department of Chemistry, Annamalai University, Annamalai Nagar-608 002, Tamilnadu, India

E-mail : drrajendiran@rediffmail.com

Manuscript received online 09 April 2016, accepted 03 October 2016

Abstract : To evaluate the role of hydrophobic and electrostatic interactions of BSA and DNA base (adenine) with two different non-steroidal anti-inflammatory drugs, [meloxicam (MEX) and piroxicam (PIR)]. Both drugs have different heterocyclic rings. The binding affinity for the protein-drug formation is found to depend primarily on the different heterocyclic rings or functional groups like OH, C=O, NH, etc. suggesting the essential role of hydrophobic forces, supported by hydrogen and polar bonding interactions at the protein surface. UV-Visible, fluorescence, IR, cyclic voltammetry and molecular docking analysis were performed to compare the effects of heterocyclic rings of two drugs on BSA/adenine. The fluorescence spectral blue shift suggested that both drug molecules strongly interacted with BSA. The difference in the IR spectrum of BSA, pure drugs and complex confirm the interactions between the drugs to BSA. With an increase the concentration of drugs, the oxidation peaks of MEX and PIR were shifted to higher potential (E_{pa}) and the oxidation peak current (I_{pa}) is also increased. These observations suggested the formation of non-electroactive interactions between BSA/adenine with drug molecules. Docking analysis showed PIR strongly interacted with BSA rather than MEX.

Keywords : BSA, meloxicam, piroxicam, fluorescence quenching, cyclic voltammetry, molecular docking.

Introduction

Non-steroidal anti-inflammatory drugs (NSAIDs) are one of the most important classes of drugs used for alleviation of pain, inflammation and fever[1,2]. Piroxicam [4-hydroxy-2-methyl-*N*-(pyridin-2-yl)-2*H*-1,2-benzothiazine-3-carboxamide 1,1-dioxide] and Meloxicam [4-hydroxy-2-methyl-*N*-(5-methyl-2-thiazolyl)-2*H*-1,2-benzothiazine- 3-carboxamide 1,1-dioxide] (Fig. 1a and b), a drug belonging to the oxicam group with enolic acid class compounds of NSAIDs, is not only a good anti-inflammatory agent, but also show chemosuppressive and chemopreventive effects in diverse cancer cell lines and animal models[3,4]. The molecular mechanism behind its anticancer effect is not yet fully understood. These drugs were strongly interacts with membrane mimetic systems like micelles and vesicles[5–8].

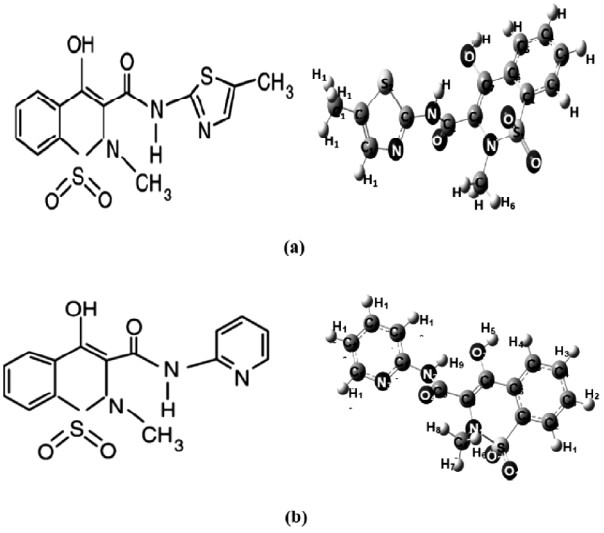

Fig. 1 Chemical and optimized structures of (a) MEX and (b) PIR.

Serum albumins, the most abundant proteins in plasma, have many physiological functions. Serum albumins often increase the apparent solubility of hydrophobic compounds in plasma and modulate their delivery to cells. Therefore, the absorption, distribution, metabolism and excretion properties, as well as the stability and toxicity of chemicals, can be significantly affected because of their binding to serum albumins. Many drugs are transported in the blood while bound to albumin. Therefore, investigation of the formation of complexes between protein and drugs is

important to know the transport and mechanism of a drug in the body[9]. Recently, it has been demonstrated that some metal complexes have high affinity for binding to human serum albumin under physiological conditions to exhibit a variety of pharmacological properties[10]. In this study, we have used bovine serum albumin (BSA) as the protein model due to its medical importance, low cast, easy availability, intrinsic fluorescence emission, and structural homology with human serum albumin (HSA)[11].

Besides DNA and RNA, adenine is also an important part of ATP. ATP is the nitrogen purine base adenine bonded to a five carbon sugar molecules. This molecule is important because it has the ability to add a phosphate (PO_4^{3-}) group to some other molecules. This transfer of a PO_4^{3-} group allows energy to be released and that energy is used by cells in living organisms. Adenine is also part of adenosine, which is important paracrine factor controlling blood flow during ischemia. ADP and ATP also affect many processes in organism acting on P2X and P2Y receptors, including aggregation of thrombocytes and smooth muscle tone. Therefore, adenine is much more interesting for research than other DNA bases. This is why the nitrogenous purine base adenine molecule is so important. From the above importance of adenine, we just tried the experimental section with adenine out of all four bases in DNA and RNA. In this study, the properties of binding between two oxicam drugs namely meloxicam (MEX) and piroxicam (PIR) with BSA and DNA base adenine were investigated using spectral (UV-Visible absorption spectroscopy, fluorescence spectroscopy), electrochemical (cyclic voltammetry) and molecular docking analysis. The aim of this study was to analyze the fluorescence quenching mechanism of BSA/adenine by oxicam drugs, the number of the binding sites, the energy transfer efficiency, the specific binding pocket, and the effects of drugs on the conformational changes of BSA and adenine. In addition, the molecular modelling was used to improve the understanding of the interaction of this drug with BSA. The principal ligand binding sites in BSA are located within site 2 (subdomain IIIA).

Experimental

Materials :

BSA, adenine, MEX and PIR were purchased from Sigma-Aldrich, USA and used without further purification. The stock solution of 1.0×10^{-3} mol L^{-1} of BSA and adenine was prepared by dissolving the solid protein in Tris-HCl buffer solution of pH ~7.4 and stored at 4° C in the dark for about a week. The working solution of BSA (1.0×10^{-5} mol L^{-1}) was prepared daily. The Tris-HCl buffer (pH ~7.4) containing 0.10 mol L^{-1} NaCl was selected to keep the pH value and maintain the ionic strength of the solution. MEX and PIR stock solutions (1.0×10^{-3} mol L^{-1}) were prepared by directly dissolving their corresponding crystals in methanol solution further it is diluted by using doubly distilled water. All other chemicals were of analytical reagent grade, and doubly distilled water was used throughout.

Apparatus :

All fluorescence spectra were recorded on a Shimadzu spectrofluorimeter model RF-5301 equipped with a thermostatic bath and a 10 mm quartz cuvette. The UV-Visible absorbance spectra were recorded on a Shimadzu UV-2600PC (Japan) using a 10 mm cuvette. The pH value was measured using an Elico pH meter model LI-120. Cyclic voltammetry measurements were performed through an electrochemical workstation (model-CHI 620D, CH Instruments, USA) with a three electrode system and the molecular docking studies were done by using molecular docking server.

UV-Visible absorption studies :

The absorption spectra of BSA and adenine in the presence and absence of two NSAI drugs were recorded at room temperature.

Fluorescence titration experiments :

The concentration of stock solution of the BSA and adenine was 2×10^{-3} *M*. The stock solution (0.2 ml) was transferred into 10 ml volumetric flasks. To this, varying concentration of above drug solution (1.0×10^{-4} to 1.0×10^{-3} *M*) was added. The mixed solution was diluted to 10 ml with triply distilled water and shaken thoroughly. The final concentration of BSA and adenine in all the flasks was 2×10^{-5} *M*. The excitation wavelength was set at 280 nm and emission spectra were recorded in the wavelength interval of 290–500 nm. The width of the excitation and emission slits were set to 10.0 and 5.0 nm, respectively, and the scanning speed was set at 1000 nm min^{-1}. The titration experiments were achieved at room temperature. Since the absorbance of MEX and PIR at higher concen-

trations introduces the inner filter effect (IFE) that decreases the fluorescence emission of BSA and hence interfere with the quenching process, the fluorescence intensities were corrected to decrease the inner filter effect according to the following relationship[12] :

$$F_{cor} = F_{obs} \times e^{(A_{ex}+A_{em})/2} \quad (1)$$

where F_{cor} and F_{obs} are corrected and observed fluorescence intensities, respectively, and A_{ex}, A_{em} are the absorption of the durgs at the excitation and the emission wavelengths of albumin, respectively.

Cyclic voltammetry :

For voltammetric studies, the concentration of BSA and adenine was maintained constant (10^{-6} *M*) while that of drugs were varied (1.0×10^{-4} to 1.0×10^{-3} *M*). Cyclic voltammetry measurements were performed through an electrochemical workstation (model-CHI 620D, CH Instruments, USA) with a three electrode system : surface area 0.1963 cm^2 glassy carbon electrode as working electrode, saturated silver electrode as reference electrode and a platinum foil as counter electrode. Prior to use, the working electrode was polished with 0.05 μm alumina and thoroughly washed in an ultrasonic bath for 5 min. Before experiments, the solution within a single-compartment cell was directed by purging with pure N_2 gas for 5 min.

Molecular docking studies :

Docking calculations were performed by using molecular docking Server (http://www.dockingserver.com)[13]. The MMFF94 force field was used for energy minimization of the both drug (MEX and PIR) molecules using Docking Server[14]. Gasteiger partial charges were added to the drug atoms. Non-polar hydrogen atoms were merged, and rotatable bonds were defined. Docking calculations were carried out on ***4F5S*** protein model. Essential hydrogen atoms, Kollman united atom type charges, and solvation parameters were added with the aid of Auto Dock tools[15]. Affinity (grid) maps of $20\times20\times20$ Å grid points and 0.375 Å spacing was generated using the Auto grid program[15]. Auto Dock parameter set- and distance-dependent dielectric functions were used in the calculation of the van der Waals and the electrostatic terms, respectively. Docking simulations were performed using the Lamarckian genetic algorithm (LGA) and the Solis & Wets local search method. Initial position, orientation, and torsions of the drug molecules were set randomly. Each docking experiment was derived from 10 different runs that were set to terminate after a maximum of 25×10^4 energy evaluations. The population size was set to 150. During the search, a translational step of 0.2 Å, and quaternion and torsion steps of 5 were applied.

Results and discussion

Absorption and fluorescence spectral studies :

Absorption and fluorescence spectra of BSA and adenine were recorded in the presence of MEX and PIR and the relevant data are listed in Table S1. Fig. S1 displays the absorption spectra of BSA and adenine as a function of different concentrations of the drugs. In water, the absorption band maximum of MEX appears at ~360, 270 and 208 nm (Fig. 2) and PIR shows at ~356, 285, 251 nm (Fig. 2). In aqueous solution, BSA and adenine, have an absorption maximum at ~280 nm and 260 nm respectively.

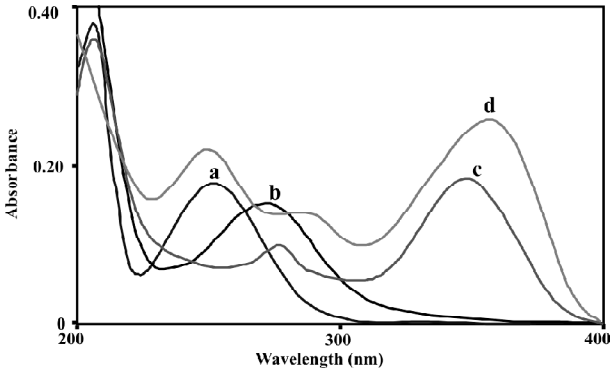

Fig. 2. Absorbance spectra of (a) adenine, (b) BSA, (c) MEX and (d) PIR.

The addition of both drug molecules in BSA and adenine leads to no significant spectral shift was observed (Fig. S1). However, with increasing the concentration of drugs, the absorption maximum of MEX and PIR was completely lost, whereas BSA and adenine absorbance was decreased at the same wavelength. These results indicate that both drugs are interacted with BSA and adenine[16–20]. The inset in Fig. S1 depicts the changes in the absorbance with drug concentrations, indicating that both drugs could bind to BSA and adenine molecules. When compared to both drugs, the absorbance of PIR-BSA is decreased more than that of MEX-BSA. Further, when recorded the absorption spectra after 24 h no significant change was ob-

served in the absorbance, indicating that both drugs do not decompose in the BSA and adenine solutions. In addition to that, a clear isosbestic point was observed in the absorption spectra, which designates the formation of well-defined 1 : 1 complex between the drugs and BSA or adenine.

Fig. 3 demonstrates the emission spectra of aqueous BSA and adenine solution containing MEX and PIR at various concentrations. The effects of BSA and adenine on the emission spectra of both molecules are more pronounced than the corresponding effect on the absorption spectra. BSA showed a more quenching effect rather than adenine.

In water, MEX and PIR exhibit two emission bands at ~470, 413 nm and 449, 410 nm ($\lambda_{excitation}$ ~360 nm) respectively. MEX and PIR can emit relatively strong fluorescence in water (excited at 360 nm) whereas both emission intensities are very low with the excitation of BSA ($\lambda_{excitation}$ ~280 nm). The introduction of an aqueous BSA solution into the drugs produced a blue shift in the emission maxima. The blue shift signified that the binding of MEX/PIR was associated with changes in the local environment in BSA. This result suggests that both drug molecules interacted with BSA and adenine[16–20].

Similarly, the adenine fluorescence intensity also gradually decreased with increasing the concentration of drugs. With an addition of drugs, the decrease in the adenine emission intensity may be due to the following reasons : (i) ground state trapping of transferable proton within the adenine molecule; the N-H proton may not be accessible to the nitrogen atom of the heterocyclic and (ii) non-radiative decay of the tautomer; interaction of drug with amine or -NH- or -N= group of the adenine molecule. This non radiative channel is expected to decrease or diminish the fluorescence intensity of the tautomer form.

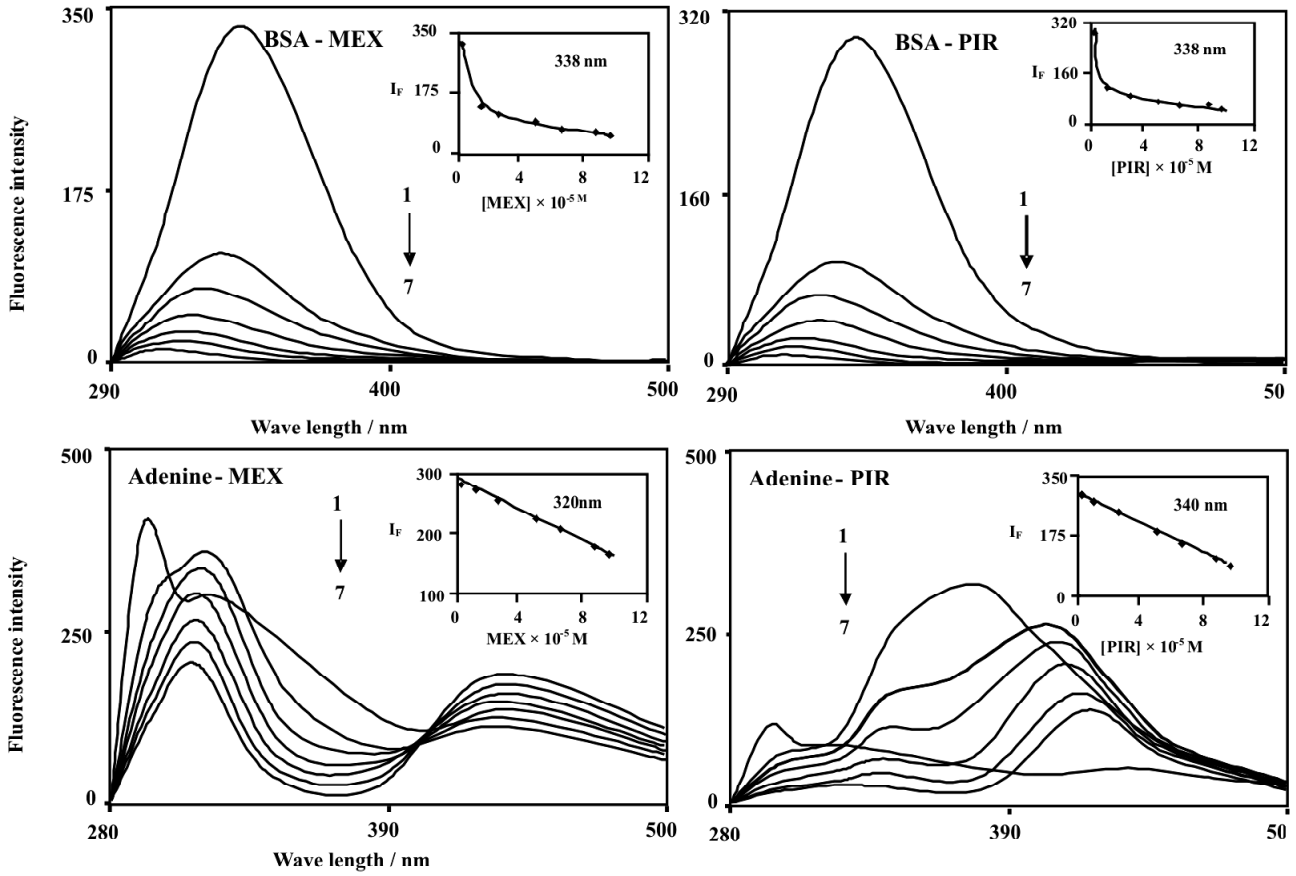

Fig. 3. Fluorescence spectra of BSA and adenine with different MEX and PIR concentrations ($\times 10^{-3}$ *M*) : (1) 0, (2) 1, (3) 3, (4) 5, (5) 7, (6) 9 and (7) 10; Inset figure : Fluorescence intensity vs drugs concentration.

Quenching mechanism :

Fig. 3 shows quenching of fluorescence intensity of tryptophan residues in BSA with increasing concentration of the drugs at pH ~7.0. It is possible to estimate the quenching of tryptophan fluorescence in the presence of the drugs using the Stern-Volmer equation. On the basis of relationship between quenching of excited states and drug concentration, the Stern-Volmer[21] quenching values calculated from the equation (S1). Fig. S2 shows the Stern–Volmer and modified Stern-Volmer plots of BSA and adenine with the drugs at pH ~7.0 and these plots are linear with increasing concentration of the drugs, suggested that single type of quenching, (i.e.) static or dynamic.

The binding constants obtained using the Stern-Volmer methods for the interactions of BSA and adenine with drugs are listed in Table 1. The bimolecular quenching constant (K_q) calculated from the slope of the plots (Figs S2). The high value of quenching rate constants implies that the quenching is static in nature (Table 1).

quenching mechanism results, PIR showed more hydrophobic nature rather than MEX. The protein-amphiphile interactions will be strongly influenced by the amphiphilic nature; that is, the charge or nature of the hydrophilic group[22]. MEX contain thiazole ring, whereas PIR comprises of pyridine ring, suggesting that the heterocyclic group may leads the interaction between the BSA/adenine with PIR and MEX. For the static quenching process, the hypothesis that BSA has the same and independent binding sites, binding constant or association constant (K_a) and the number of binding sites (n) was determined by using equation (S2).

Binding constant and the number of binding sites for the BSA and adenine systems can be obtained by the plot log $[(F_0 - F)/F]$ versus log $[Q]$ as shown in Fig. S2c. From the slope of the linear fitting plots, number of binding sites (n) and from the intercept (log K_a), the binding constants (K_a), were calculated are given in Table 1. The values of n indicate that in each case the probe is located

Table 1. Stern-Volmer quenching constant (K_{sv}) and modified Stern-Volmer association constant (K_a) and bimolecular quenching rate constant (K_q) of the BSA and adenine with MEX and PIR systems at 300 K

		Drugs	K_{sv} (10^5 M^{-1})	K_q (10^{13} M^{-1} s^{-1})	R^a	SD
S-V quenching	BSA	MEX	1.317	1.317	0.990	0.592
		PIR	1.399	1.399	0.991	0.765
	Adenine	MEX	0.889	0.889	0.999	0.398
		PIR	1.077	1.077	0.999	0.599
	BSA	Drugs	K_a (10^5 M^{-1})	ΔG^0 (kJ/mol)	n	R^a
Modified S-V quenching		MEX	2.383	–21.70	0.99	0.99
		PIR	2.414	–22.64	1.04	0.99
	Adenine	MEX	0.895	–20.02	0.76	0.99
		PIR	1.915	–21.34	0.87	0.99

R^a – Linear correlation coefficient. SD – Standard deviation.

The maximum value of K_q for diffusion controlled quenching process[22] with biopolymer is about 2.0×10^{10} M^{-1} s^{-1}. The larger value of K_q for the BSA-drugs compared to that for the adenine-drugs indicates less quenching in the latter. Static quenching suggests the presence of interaction between BSA and PIR/MEX drugs. The changes in the fluorescence intensity (Fig. 3) show that the environment of tryptophan is highly affected during the interaction with the MEX and PIR. The blue-shift of λ_{max} and the increase in K_{sv} suggests strong interaction between BSA with PIR than that of BSA with MEX. From the

at only one binding site. The binding constant obtained for the drugs with BSA/adenine suggests lower binding affinity compared to other strong protein-ligand complexes (binding constants ranging from 10^6 to 10^8 M^{-1}). However, lower binding constants (10^3–10^5 M^{-1}) were reported for several other protein-ligand complexes[22–25]. Table 1 shows binding constant (K_{sv}, K_q and K_a) values for both drugs with BSA and adenine. The K_{sv} value of PIR with BSA/adenine is high as compared to MEX with BSA and adenine.

The K_a value is important for recognition of the me-

tabolism, distribution and delivery of ligands (drugs). A small binding constant can increase the concentration of free drug in the plasma and causes a short lifetime or a poor distribution. Also, a large binding constant can decrease the concentration of free drug in the plasma and improves the pharmacological effects[26,27]. The value of n is more or less equal to 1, indicating the presence of one binding site in BSA and adenine for the complex[28]. In other words, the drugs with BSA and adenine form a complex with a molar ratio 1 : 1[29]. The free energy change was calculated from the binding constant (K_a) by using the following equation :

$$\Delta G_0 = -RT \ln k \quad (2)$$

The ΔG^0 values for MEX and PIR with BSA/adenine are given in Table 1. As can be seen from the Table, ΔG^0 is negative, which suggests that these quenching interactions proceeded simultaneously at 300 K. The experimental results indicate that the binding reactions of the BSA and adenine with the drugs are an exothermic process.

FRET study :

Forster's non-radioactive energy transfer (FRET) theory is used to determine the distance between the protein and the drugs in the binding site[30]. The energy transfer takes place under three conditions : (1) The presence of a fluorophore donor, (2) a sufficient overlap between the emission spectrum of the donor species and the UV-Vis spectrum of the acceptor species, (3) the donor species are near to the acceptor (the distance is less than 8 nm)[31].

According to the FRET, the energy transfer efficiency (E) [equation (S4)] is related to the distance between the acceptor and donor pair (r) and the critical energy transfer distance (R^0)[32]. According to equations (S3)-(S5) and the experimental data for BSA with MEX and PIR (Table S1) the values of, J = 1.77, 2.01 (10^{-14} cm^3 L mol^{-1}), E = 0.39, 0.47, R^0 = 0.92, 0.96 (nm), and r = 0.84, 0.91 (nm) were calculated. The value of r is less than 8 nm, and $0.5R^0 < r < 1.5R^0$, indicating the energy transfer from BSA/adenine to the drugs occurs with high probability[33–35]. Table S1 shows the energy transfer efficiency (E) values for MEX with BSA and adenine has more efficiency than PIR with BSA/adenine molecules.

ATR-IR spectral studies :

The protein-ligand complex formation has been further confirmed by IR spectroscopy, because the bands resulting from the interaction part of the drug molecule are generally shifted or their intensities altered (Fig. 4). The IR peaks of pure BSA at 3354, 2974, 1649, and 1540 cm^{-1} are assigned to the stretching vibration of -OH, amide I (mainly -NH stretching vibration), amide (mainly C=O stretching vibrations) and amide II (the coupling of bending vibrate of N-H and stretching vibrate of C-N) bands, respectively.

In pure MEX (Fig. 4b), NH, C=O, C-C, and two S=O stretching vibration peaks were obtained at 3291, 1621, 1558, 1346 and 1161 cm^{-1} respectively. In BSA-MEX (Fig. 4d), the NH band shifted from 3291 to 3386 cm^{-1} and the stretching vibration of the amide C=O moved to 1646 cm^{-1}. The two stretching bands of the SO_2 group also shifted to lower frequencies due to hydrogen bonding effect which confirm the interaction between BSA and MEX.

In pure PIR, the OH, C=O, and S=O, stretching vibration frequency appear at 3376, 1708, and 1354 cm^{-1} (Fig. 4c). These bands were slightly shifted to the regions of 3297, 1643, and 1404 cm^{-1} in the BSA-PIR (Fig. 4e). Amide band I shifted from 1649 to 1646 cm^{-1} and 1643 cm^{-1} in MEX and PIR and amide band II moved from 1545 to 1538 cm^{-1} and 1563 cm^{-1} in MEX and PIR respectively. The difference in the IR spectrum of BSA, pure drugs and complex confirms the interactions between the drugs to BSA.

Cyclic voltammetry :

The cyclic voltammetric (CV) technique has been used to find out the interaction of the drugs with protein in order to confirm the protein bonding modes. The oxidation peaks of isolated MEX and PIR showed at 0.566 and 0.749 V in pH ~7.4 (Fig. S3). In order to investigate the interaction of both drugs with BSA or adenine, known concentrations of drug were added to fixed concentration of BSA and adenine solution and the CV were recorded and the values are given in Table 2.

With an increase the concentration of drugs, the oxidation peak current (I_{pa}) of MEX with BSA is decreased whereas I_{pa} is increased in PIR-BSA and a positive shift of electrode potential (E_{pa}) is obtained. Similarly, in adenine system, both oxidation peaks of MEX and PIR were shifted to higher potential with increase in I_{pa}. The above observations suggested the formation of non-electroactive

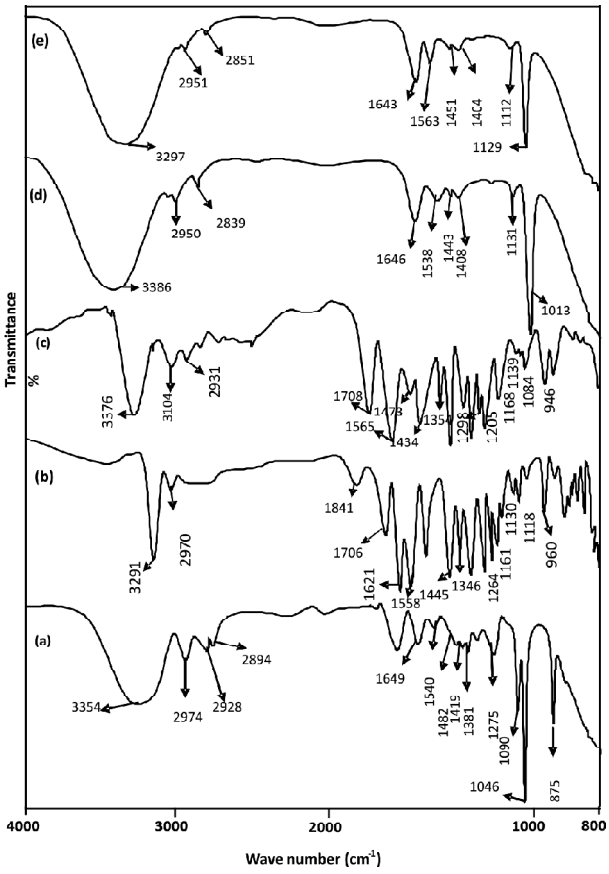

Fig. 4. IR spectra of (a) BSA, (b) MEX, (c) PIR, (d) MEX-BSA and (e) PIR-BSA.

interactions between BSA/adenine with drug molecules. Further, it was proposed that the decrease in peak current is mainly due to decrease in free concentration of drugs and formation of complex between drugs and protein. But it is not due to the factors like, (i) alteration in the electrochemical kinetics of the drugs, (ii) addition of BSA or the blockage of the electrode surface, (iii) adsorption of BSA/adenine on the electrode, (iv) competitive adsorption between drugs and protein on GCE. The observed potential shift in the oxidation peak was attributed to hydrophobic interaction between the drugs and protein[36].

An electrostatic binding mode between organic molecules and bio molecules (protein) causes a more negative shift in the formal potential (E_0), while an intercalative binding mode results in an E_0 shift to a more positive potential[37]. Consequently, both drugs can interact with BSA and adenine through a partial intercalative binding mode. Further, the voltammograms of the drug : BSA interactions were collected at the different scan rates (Fig. 5).

Plot of E_p vs υ and E_p vs ln υ is given well-defined straight line (Fig. 6a and Fig. 6b). From this plot, αn value can be calculated from the slope and k_s from the intercept. E_0 value can be deduced from the intercept of E_p vs υ plot on the ordinate by extrapolating the line to $\upsilon = 0$, when υ was approached to zero, then E_p was approached to E_0. The number of binding sites (n) and binding constant (β_s) of electrochemical interaction between BSA/adenine with drugs are deduced by the eq. (3).

$$\log [\Delta I/[\Delta I_{max} - \Delta I] = \log \beta_s + m \log [\text{drugs}] \quad (3)$$

where ΔI is the peak current difference between the presence and absence of BSA and ΔI_{max} corresponds to the obtained value when the concentration of drugs is extremely higher than that of BSA. C_{BSA}, [BSA], [BSA-m_{drugs}] are corresponding to the total, free and bound concentration of protein in the solution, respectively. The plot of log [$\Delta I/(\Delta I_{max} - \Delta I)$] vs log [$Q$] shows linearity indicates the drugs form a single complex with BSA or adenine (Fig. 6c). The binding ratio and binding constant values are obtained from the slope and intercept of this plot. The value of binding constant is in close agreement with that obtained by spectroscopic techniques.

Molecular docking analysis :

The molecular docking study was performed to further reveal the interaction of MEX and PIR with BSA. The major principal regions of ligand binding to BSA are located in hydrophobic cavities in sub-domains IIA and IIIA, and these are consistent with Sudlow sites I and II, respectively. In the present study, the molecular docking server program was applied to calculate the possible confirmation of the MEX and PIR that binds to the BSA. The crystal structure of BSA was obtained from the Protein Data Bank (PDB code ***4F5S***)[16–20]. The best energy ranked results are summarized in Table 3.

Fig. 7 shows that the best binding mode between (Fig. 7a) MEX and (Fig. 7b) PIR with BSA. The important residues of BSA are represented using "surface" format and the ligand (drug) structure is represented using a "Ball and Stick" format (colour of the atoms : skeleton structure – BSA, blue – nitrogen, red – oxygen, yellow – sulphur, green – carbon). The hydrogen bonding and hydrophobic interaction plots between drugs MEX and PIR with BSA are shown in Fig. 7c and Fig. 7d respectively. In that plot, BSA residues are represented using black

Table 2. CV for BSA and adenine with drugs (scan rate, 100 mV s^{-1}, concentration of BSA and adenine – 2×10^{-6} *M*; drugs concentration : 0, 3, 5, 7 and 10×10^{-3} *M*)

Drug-BSA or adenine	Drug concentration × 10^{-3}	E_{pa}	I_{pa}	E_{pc}	I_{pc}	$E_{pa} - E_{pc}/2$	I_{pa}/I_{pc}
BSA only	2×10^{-6}	973	0.524	–	–	487	–
MEX only	2	763	0.566	–	–	381	–
BSA-MEX	3	776	0.672	–	–	388	–
	5	785	0.637	–	–	392.5	–
	7	819	0.628	–	–	409.5	–
	10	844	0.591	–	–	422	–
PIR only	2	800	0.749	–	–	400	–
BSA-PIR	3	893	0.556	–	–	446.5	–
	5	1010	0.924	–	–	505	–
	7	1069	1.089	–	–	534.5	–
	10	1116	1.253	–	–	558	–
Adenine only	2×10^{-6}	987	0.613	–	–	678	–
Adenine-MEX	3	793	0.922	–	–	396.5	–
	5	773	0.880	–	–	386.5	–
	7	826	0.852	–	–	413	–
	10	969	0.720	–	–	484.5	–
Adenine-PIR	3	773	1.068	–	–	386.5	–
	5	796	0.876	–	–	398	–
	7	858	0.825	–	–	429	–
	10	926	0.813	–	–	463	–

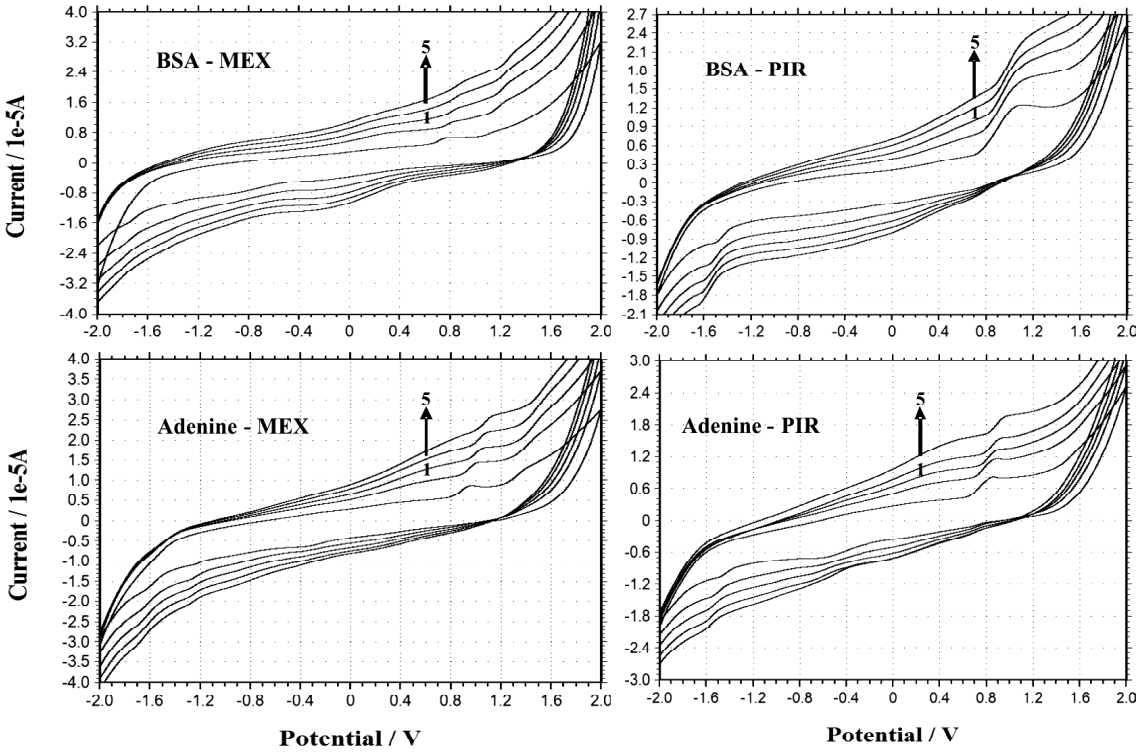

Fig. 5. Cyclic voltammograms of a carbon electrode in BSA and adenine with successive additions of a final concentration of drugs (MEX and PIR) with different scan rate = (100–500 mV s^{-1}).

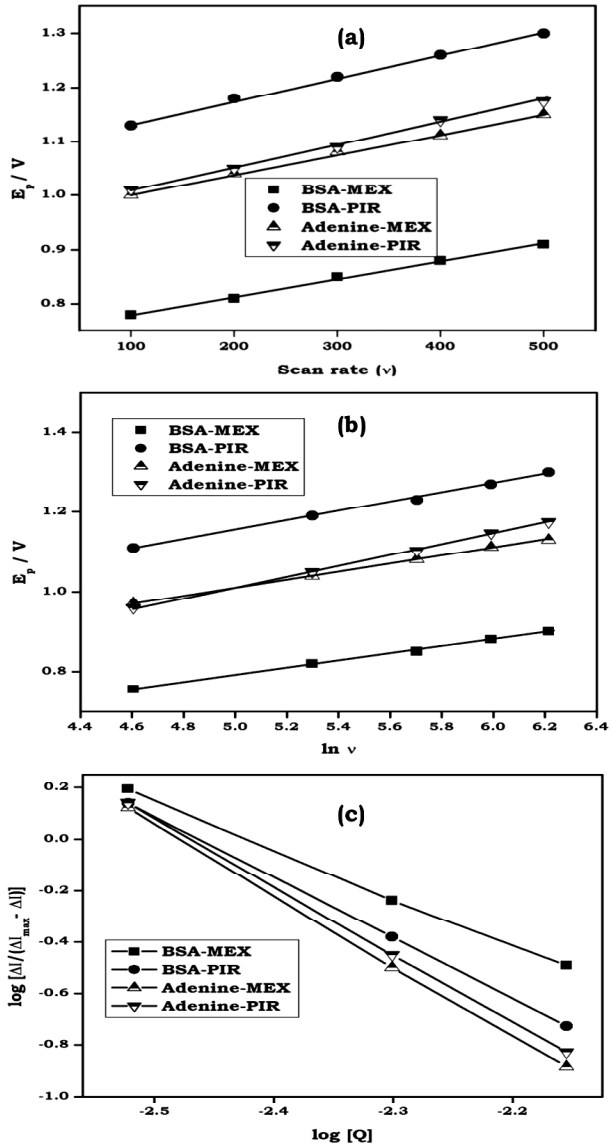

Fig. 6. [a] Dependence of the peak potential (E_p) on scan rate (ν), [b] Semilogarithmic dependence of the peak potential (E_p) on scan rate (ln ν), and [c] Linear plot of log [Q] vs log [$\Delta I/(\Delta I_{max} - \Delta I$] of drugs with BSA and adenine.

dots and the hydrogen bonding and hydrophobic interactions are represented using red dots. The Leu397, Tyr400, Glu540, Leu543, Met547, Val551 and Asn404 of site II are involved in hydrophobic interaction between MEX and BSA (Table S2). Similarly, in the PIR-BSA interaction, Phe501, Phe506, Phe508, Phe550, Ala527, Leu528, Leu531, Leu574, Val546, Val575, Thr578 and Met547 were very crucial residues present at the active site (Tables S3).

Fig. 8 shows, two-dimensional and three-dimensional schematic representation of hydrogen bonding and hydrophobic interactions of BSA with MEX and PIR (active residues are represented in green colour sweeps; colour of the atoms : blue – nitrogen, red – oxygen, yellow – sulphur, black – carbon). The list of interactions between BSA and drugs (MEX and PIR) are listed in Tables S2 and S3. The drug (PIR) core was interacted with the protein through the H-bonds. In PIR, the sulfonyl oxygen atoms (O_1) form H–bond with the group of Thr578 (–O·····HO, 2.77 Å) but MEX not form H-bonds with BSA (Tables S2 and S3, Fig. 8). The above results showed MEX have more hydrophobic nature than PIR. This may be due to the presence of different heterocyclic ring in both drugs (thiazole ring present in MEX and pyridine present in the PIR).

The binding constant of the MEX and PIR to BSA found to be –4.80 and –5.70 kcal/mol respectively. The docking study also shows that the distance between Thr578 residue and the sulfonyl oxygen group of PIR is 2.77 Å this finding provides a good agreement with the fluorescence quenching of BSA emission in the presence of the MEX and PIR drugs. This result is in agreement with the observation made by spectroscopic techniques. So, it is proposed that the interaction occurred between the hydro-

Table 3. Estimated free energy, inhibition constant, electrostatic energy and total intermolecular energy of the BSA with MEX and PIR

Drug	Est. free energy of binding (kcal/mol)	Est. inhibition constant, K_i (μM)	vdW+H bond + desolv energy (kcal/mol)	Electro static energy (kcal/mol)	Total inter molecular Energy (kcal/mol)	Frequency (%)	Interact. surface
MEX	–4.80	304.9	–5.31	+0.01	–5.30	20	854.5
PIR	**–5.70**	**66.70**	**–6.34**	–0.02	–6.36	40	698.8

The strong interactions are mentioned in the bold letters.

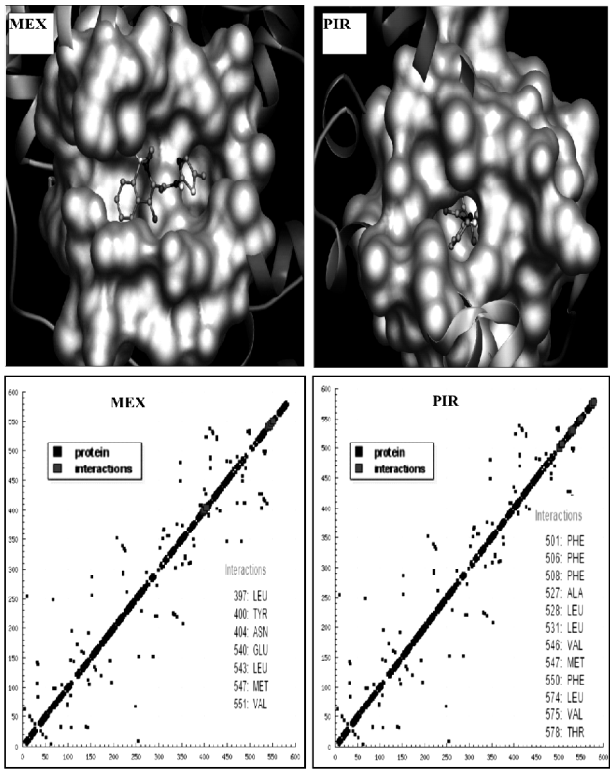

Fig. 7. Best binding mode between drugs (a) MEX and (b) PIR with BSA. The important residues of BSA are represented using "surface" format and the ligand (drug) structure is represented using a "Ball and Stick" format. The hydrogen bonding plots between drugs. Color of the atoms : Surface structure – BSA, blue – nitrogen, red – oxygen, yellow – sulphur, green – carbon. The hydrogen bonding plots between drugs with BSA. The BSA residues are represented using black dots and the hydrogen bonding interactions are represented using red dots.

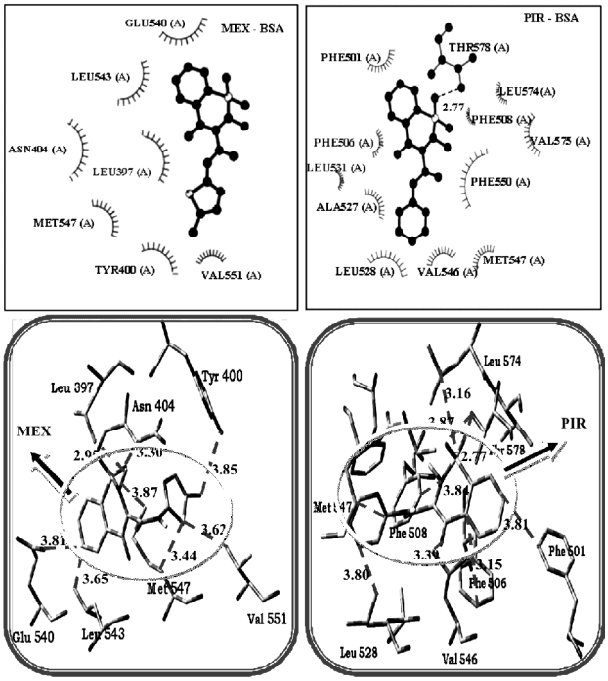

Fig. 8. Two-dimensional schematic representation of hydrogen bonding and hydrophobic interactions of BSA with MEX and PIR. Active residues are represents in green colour sweeps. Colour of the atoms : blue – nitrogen, red – oxygen, yellow – sulphur, black – carbon. Three-dimensional schematic representation of hydrogen bonding, hydrophobic, polar and π-π interactions of BSA with MEX and PIR.

phobic segment of the drug molecules and the hydrophobic part of the BSA cavity. Therefore, molecular docking yields useful information about the specific residues of BSA involved in the interactions with the both drugs for better understanding of the protein-ligand interaction at the molecular level.

Conclusion

The binding of MEX and PIR with BSA/adenine was investigated using UV-Visible, fluorescence, cyclic voltammetry and molecular docking methods. The results showed that BSA has a higher binding affinity to PIR than MEX. The fluorescence spectral blue shift suggested that both drug molecules strongly interacted with BSA. The difference in the IR spectrum of BSA, pure drugs and complex confirm the interactions between the drugs to BSA. With an increase the concentration of drugs, the oxidation peaks of MEX and PIR were shifted to higher potential (E_{pa}) and the oxidation peak current (I_{pa}) is also increased. These observations suggested the formation of non-electroactive interactions between BSA/adenine with drug molecules. Docking analysis showed PIR strongly interacted with BSA rather than MEX. Molecular docking yields useful information about the specific residues of BSA involved in the interactions with the drugs for better understanding of the protein-ligand interaction at the molecular level. The binding constant of the MEX and PIR to BSA found to be –4.80 and –5.70 kcal mol^{-1} respectively. The binding constant of BSA-PIR has more negative as compared to BSA-MEX suggests PIR has more affinity to bind BSA active site as compared to MEX molecule.

Acknowledgement

This work was supported by the Council of Scientific Industrial Research [No. 01(2549)/12/EMR-II], New Delhi, India and the University Grants Commission [F. No. 41-351/2012 (SR)], New Delhi, India.

Supplementary data

Supplementary data associated with this article can be found in the online version.

References

1. P. Luger, K. Daneck, W. Engel, G. Trummlitz and K. Wagner, *Eur. J. Pharm. Sci.,* 1996, **4**, 175.
2. M. B. Sporn and N. Suh, *Carcinogenesis*, 2000, **21**, 525.
3. S. R. Ritland and S. J. Gendler, *Carcinogenesis*, 1999, **20**, 51.
4. E. M. Grossman, W. E. Longo, N. Panesar, J. E. Mazuski and D. L. Kaminshi, *Carcinogenesis*, 2000, **21**, 1403.
5. H. Chakraborty, R. Banerjee and M. Sarkar, *Biophys. Chem.,* 2003, **104**, 315.
6. H. Chakraborty, S. Roy and M. Sarkar, *Chem. Phys. Lipids*, 2005, **138**, 20.
7. H. Chakraborty and M. Sarkar, *Langmuir*, 2004, **20**, 3551.
8. H. Chakraborty and M. Sarkar, *Biophys. Chem.*, 2005, **117**, 79.
9. P. Sathyadevi, P. Krishnamoorthy, M. Alagesan, K. Thanigaimani, P. T. Muthiah and N. Dharmaraj, *Polyhedron*, 2012, **31**, 294.
10. F. Arjmand, P. Tewatia, M. Aziz and R. H. Khan, *Med. Chem. Res.,* 2010, **19**, 794.
11. S. L. Zhang, G. L. V. Damu, L. Zhang, R. X. Geng and C. H. Zhou, *Eur. J. Med. Chem.,* 2012, **55**, 164.
12. J. R. Lakowicz, Springer Science + Business Media, New York, 2006.
13. Z. Bikadi and E. Hazai, *J. Chem. Inf.,* 2009, **1**, 1.
14. T. A. Halgren. *J. Comput. Chem.,* 1998, **17**, 490.
15. G. M. Morris and D. S. Goodsell, *J. Comput. Chem.*, 1998, **19**, 1639.
16. N. Rajendiran and J. Thulasidhasan, *Spectrochim. Acta (A),* 2015, **144**, 183.
17. N. Rajendiran and J. Thulasidhasan, *Canadian Chemical Transactions*, 2015, **3**, 291.
18. N. Rajendiran and J. Thulasidhasan, *Inter. Lett. Chem. Phys. Astro.,* 2015, **59**, 170.
19. N. Rajendiran and J. Thulasidhasan, *J. Mol. Liq.*, 2015, **212**, 857.
20. N. Rajendiran and J. Thulasidhasan, *Luminescence : J. Bio. Chem. Luminescence*, 2016, **31**, 611.
21. J. R. Lakowicz, "Principles of Fluorescence Spectroscopy", 2nd ed., Kluwer Academic/Plenum Publishers, New York, 1999.
22. D. Wu, G. Xu, Y. Sun, H. Zhang, H. Mao and Y. Feng, *Biomacromolecules*, 2007, **8**, 708.
23. W. He, Y. Li, C. Xue, Z. Hu, X. Chen and F. Sheng, *Bioorg. Med. Chem.*, 2005, **13**, 1837.
24. C. Dufour and O. Dangles, *Biochim. Biophys. Acta,* 2005, **1721**, 164.
25. C. N. Nsoukpoe-Kossi, M. R. Sedaghat-Herati, C. Ragi, S. Hotchandani and H. A. Tajmir-Riahi, *Int. J. Biol. Macromol.,* 2007, **40**, 484.
26. P. Bourassa, S. Dubeau, G. M. Maharvi, A. H. Fauq, T. J. Thomas and H. A. Tajmir-Riahi, *Eur. J. Med. Chem.,* 2011, **46**, 4344.
27. Z. Cheng, *Spectrochim. Acta (A),* 2012, **93**, 321.
28. X. L. Han, F. F. Tian, Y. S. Ge, F. L. Jiang, L. Lai, D. W. Li, Q. L. Yu, J. Wang, C. Lin and Y. Liu, *J. Photochem. Photobiol. (B),* 2012, **109**, 1.
29. X. Yu, Y. Yang, X. Zou, H. Tao, Y. Ling, Q. Yao, H. Zhou and P. Yi, *Spectrochim. Acta (A)*, 2012, **94**, 23.
30. T. Forster and O. Sinanoglu, "Modern Quantum Chemistry", Academic Press, New York, 1965.
31. Y. Zhang, S. Shi and M. Peng, *J. Lumin*, 2012, **132**, 1921.
32. L. Cyril, J. K. Earl and W. M. Sperry, "Biochemists Handbook", E. & FN Epon, Led. Press, London, 1961.
33. B. Valeur, "Molecular Fluorescence : Principles and Applications", Wiley, New York, 2001.
34. F. Samari, M. Shamsipur, B. Hemmateenejad, T. Khayamian and S. Gharaghani, *Eur. J. Med. Chem.,* 2012, **54**, 255.
35. N. Shahabadi, M. Maghsudi and S. Rouhani, *Food Chem.*, 2012, **135**, 1836.
36. H. Heli, N. Sattarahmady, A. Jabbari, A. A. Moosavi-Movahedi, G. H. Hakimelahi and F. Y. Tsai, *J. Electroanal. Chem.*, 2007, **610**, 67.
37. M. T. Carter, M. Rodríguez and A. J. Bard, *J. Am. Chem. Soc.*, 1989, **111**, 8901.